BEATS

Workpackage 3

The X-ray Source

Report on the final design of the photon source

D 3.2

July 2020

PROJECT DETAILS

PROJECT ACRONYM
BEATS

PROJECT TITLE
BEAmline for Tomography at SESAME

GRANT AGREEMENT NO:
822535

THEME

START DATE
2019

DELIVERABLE DETAILS

WORK PACKAGE: 03

EXPECTED DATE: 31/07/2020

WORK PACKAGE TITLE: THE X-RAY SOURCE

DELIVERABLE TITLE:REPORT ON THE FINAL DESIGN OF THE PHOTON SOURCE

WORK PACKAGE LEADER: INFN

DELIVERABLE DESCRIPTION: REPORT

DELIVERABLE ID: D3.2

PERSON RESPONSIBLE FOR THE DELIVERABLE: A. GHIGO

NATURE

☒ R - Report ☐ P - Prototype ☐ D - Demonstrator ☐ O – Other

DISSEMINATION LEVEL

☒ P - Public
☐ PP - Restricted to other programme participants & EC:
☐ RE - Restricted to a group
☐ CO - Confidential, only for members of the consortium

REPORT DETAILS

VERSION: 2

DATE: 31/07/2020

NUMBER OF PAGES: 30

DELIVERABLE REPORT AUTHOR(S):
A. GHIGO, J. CAMPMANY, S. GUIDUCCI, J CHAVANNE

FOR MORE INFO PLEASE CONTACT: ANDREA.GHIGO@LNF.INFN.IT

STATUS

☐ Template ☐ Draft
☒ Final ☒ Released to the EC

Table of Contents

INTRODUCTION

One of the tasks of BEATS' work package 3 is to perform design studies for an optimal X-ray source for SESAME, exploiting established concepts for a super-bend, a multipole wiggler, or a 3-pole wiggler source.

In deliverable D3.1 a comparison between the aforementioned options was made, based on presentations given at the BEATS kick-off meeting (held in March 2019) [1, 2] and on work done in the following months by the members of work package 3. Already at the BEATS kick-off meeting it was decided that a 3-pole wiggler installed in a straight section is preferred with respect to a super-bend in the arc or a multipole wiggler.

The final choice on the type of 3-pole wiggler was made in September 2019 [3]. Two different options where considered:

- The design of a 3-pole, 3 T wiggler proposed by J. Campmany (ALBA) [4] which consists of a central dipole with very intense magnetic field that acts as a super-bend and two longer poles with lower magnetic field, which act as correctors to restore the nominal electron orbit in the ring. Three versions with successive refinement have been studied during the year 2019 with the aim to minimize both the effects of the device on the electron beam dynamics (reduction of spurious multipole components) and on the infrastructure (reduction of the attractive forces). In what follows only the final (optimised) version, which will as well be the subject of the tender, will be described.
- An existing assembly from ESRF which is no longer used there and could be adapted to the BEATS beamline. This assembly was built in 1999, installed at the ESRF beamline ID15 in 2001 and removed in 2008. The material (magnet blocks and mechanical parts) could serve as a starting point to build a device similar to the aforementioned 3-pole wiggler (with the advantage of cost savings). Furthermore, the components of the assembly could as well be used to build a so-called 2-pole wiggler. This concept consists of one strong 3T super-bend deviating the electron beam horizontally, followed by another super-bend, deviating the electron beam back to its original direction, leaving just a horizontal displacement which can be compensated by steerers placed downstream. The combined photon emission of both super-bends then constitutes the x-ray source.

In this paper we present an evaluation of the aforementioned options and a detailed design of the finally chosen concept.

THE ALBA 3-POLE WIGGLER DESIGN

The conceptual model

The main design boundary parameters for the model are:

- Minimum gap: 11 mm
- Maximum field: ~ 3 T
- Magnetic length: < 1 m.
- Spectral range achieved with flux > 10^{11} [ph/s.mm^2.mrad^2.0.1%BW] in 20-50 keV photon energy range

A magnetic model for the 3-pole wiggler was generated using the RADIA code, taking into account the parameters given in the introduction [2]. This model was then refined to reduce the resulting multipolar terms and the attractive forces involved. The final model is shown in Figure 1 below. It allows reducing the required remnant field of the individual magnetic blocks down to 1.28 T, thus making the magnetic material procurement easier and cheaper. The achieved peak field is 3.0025 T.

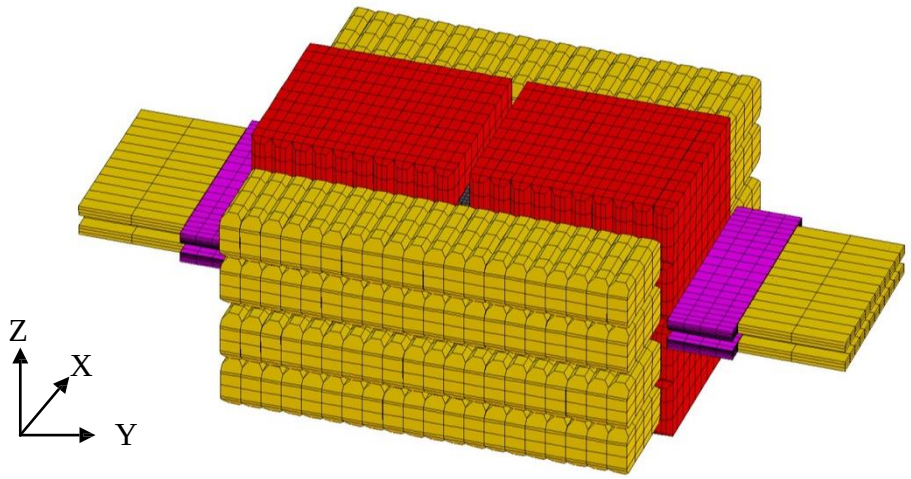

Figure 1: Axis definition and magnetic model generated by RADIA. Red and yellow parts are NdFeB magnets. Pink parts are iron poles (there is another iron pole (grey) in the centre). The overall length is 0.755 m, the overall width and height are 0.400 m and 0.331 m, respectively. The minimum gap is 11 mm.

This design has three major advantages:

- The magnetic force is compensated and decreased to a very low value of **1245.22 N**
- The magnetic field is concentrated in the central part and, consequently, the central field is enhanced. Therefore, one can build the device using magnetic material with lower remanence and higher coercitivity than those used in former versions.
- No side blocks are needed.

Figure 2 shows the field lines in the gap of the 3-pole wiggler.

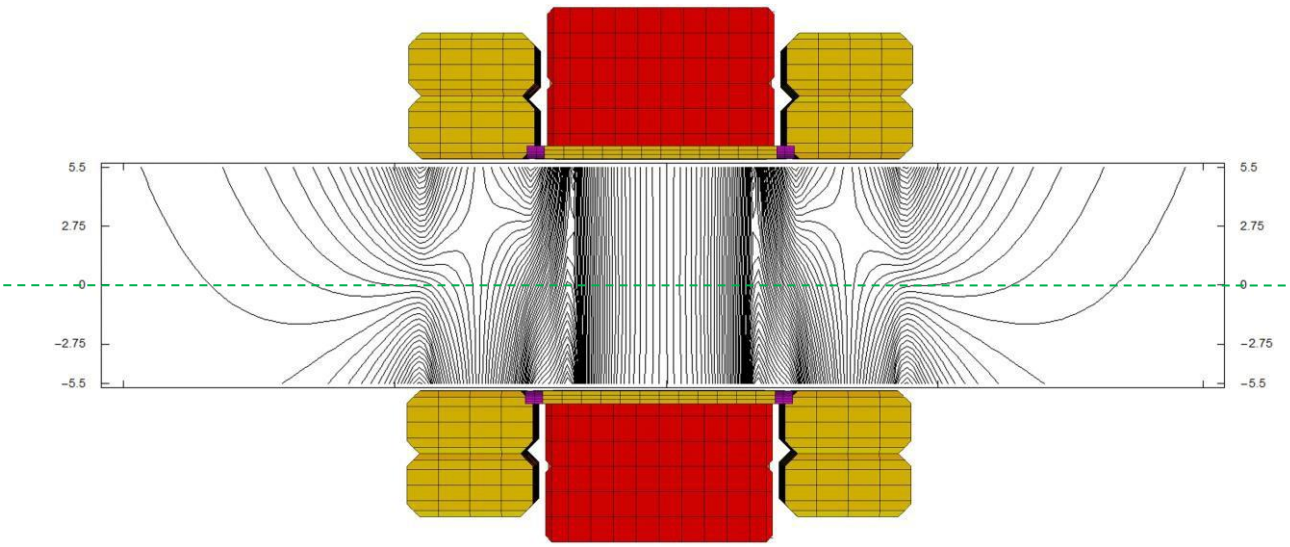

Figure 2: Magnetic field lines within the gap at longitudinal position Y=0.

In order to optimize the design, it was assumed that the mechanical tolerances of magnetic blocks and iron poles in longitudinal axis are ±0.020 mm. This means that the void (also referred to as “air gap”) left between blocks and poles to allow for fabrication tolerances should be 20 µm. (Figure 3).

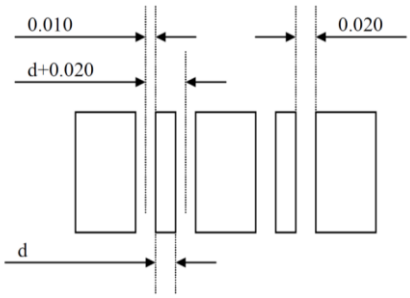

Figure 3: Schematics of pole / block arrangement and air gaps left for tolerances

All permanent magnets are made of the same material with the remnant field B_r =1.28 T. The orientation of the magnetization orientation is shown in Figure 4 below.

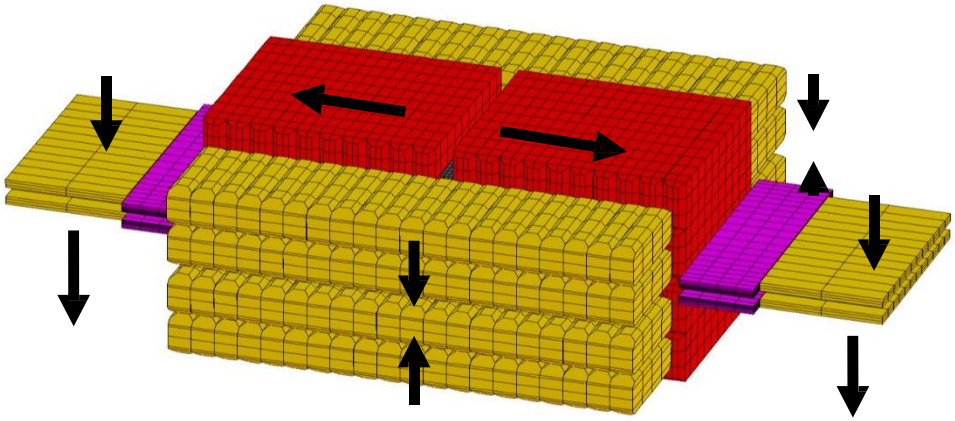

Figure 4: Magnetization directions in the assembly of 3PW.

The design has been optimized to obtain a low first field integral, low attractive force and low decapole components. Table 1 lists the longitudinal position and size of each block

Position (mm)	Magnetic structure	Length (mm)	B_r orientation
-377.5	Edge block	105	(0,0,-1) top and bottom
-272.5	Air gap	0.5	-
-272.0	Iron (permendur)	64	-
-208.0	Air gap	0.5	-
-207.5	10 magnetic blocks	200	(0,-1,0) top (0,1,0) bottom
-7.5	2 Side blocks	15	(1,0,0) and (-1,0,0)
-7.5	Iron (permendur)	15	-
7.5	10 magnetic blocks	200	(0,1,0) top (0,-1,0) bottom
207.5	Air gap	0.5	-
208.0	Iron (permendur)	64	-
272.0	Air gap	0.5	-
272.5	Edge block	105	(0,0,-1) top and bottom
377.5	End of device	-	-
-50.0	20 Lateral blocks	400	(0,0,±1) opposite top and bottom

Table 1: Description of the magnetic arrangement

The magnetic field along the electron beam and along the transversal axis (roll-off) is shown in Figure 5 and 6, respectively.

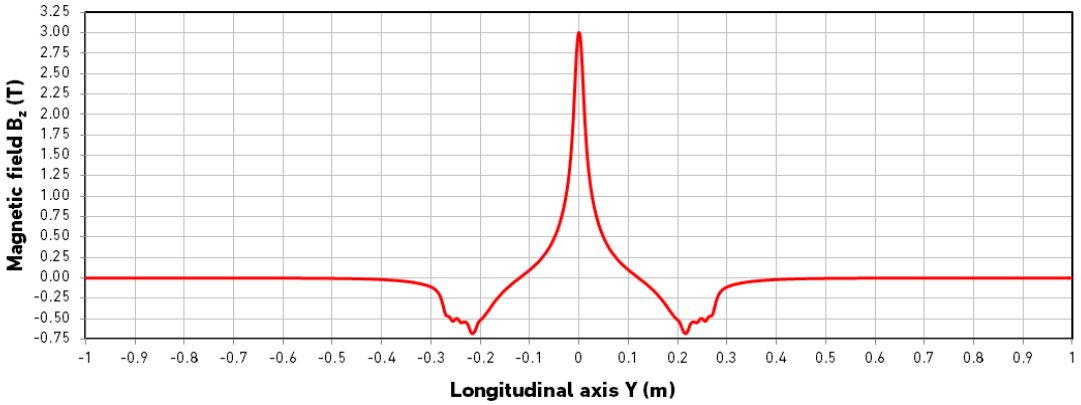

Figure 5: Magnetic field Bz on axis.

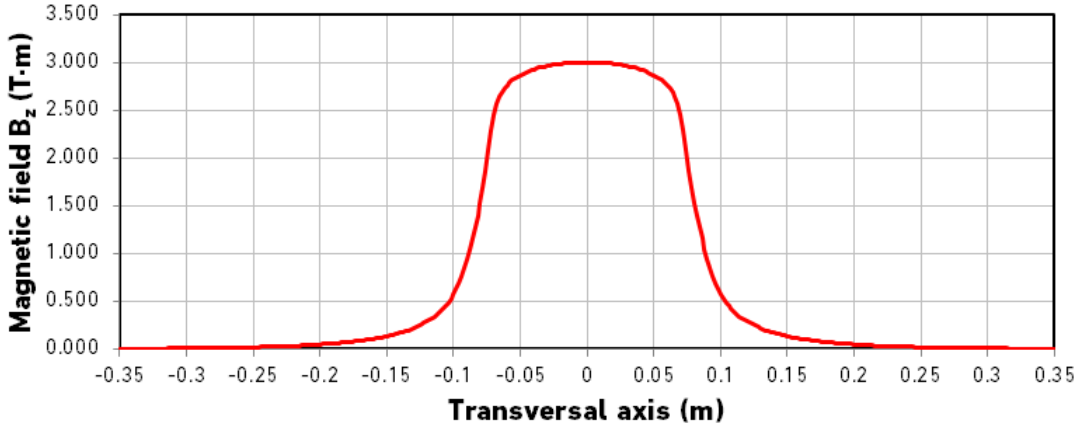

Figure 6: Magnetic field Bz along the transversal axis.

A 3D field-map in the symmetry plane is presented in Figure 7. (Peak field: 3.0025 T)

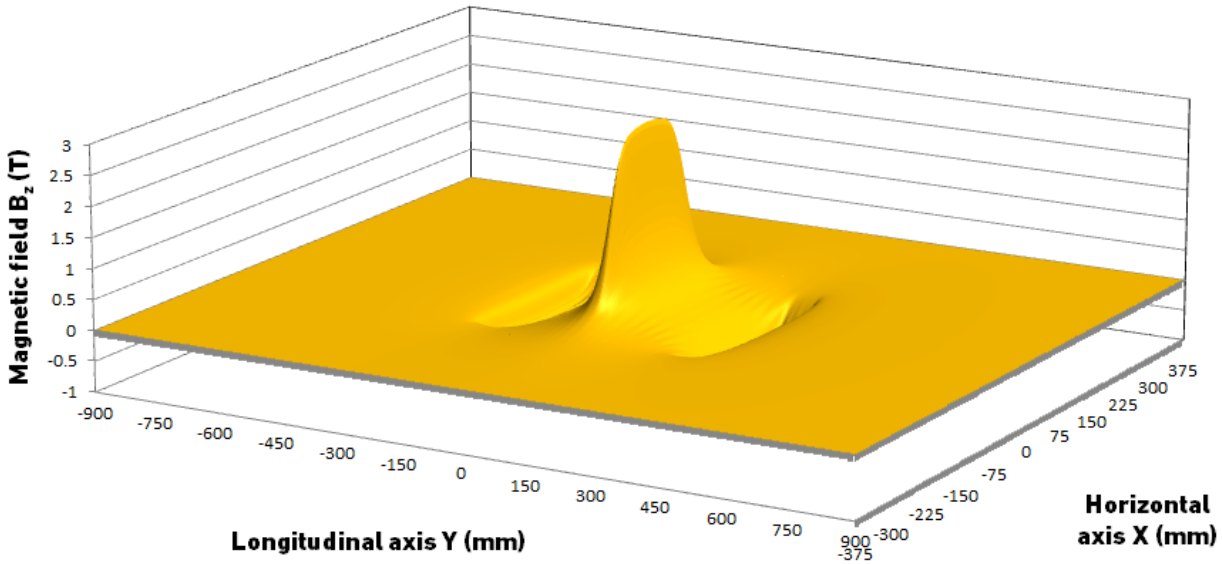

Figure 7: 3D Map of the vertical field Bz in the 3-pole wiggler.

The computed velocity and electron trajectory is shown in Figures 8 and 9, respectively, below.

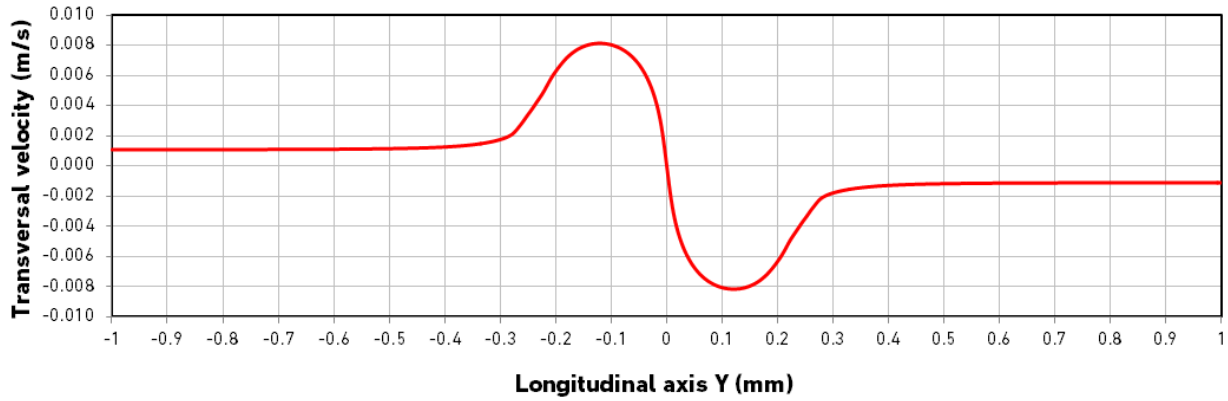

Figure 8: Map of the transversal velocity of electrons along the 3-pole-wiggler.

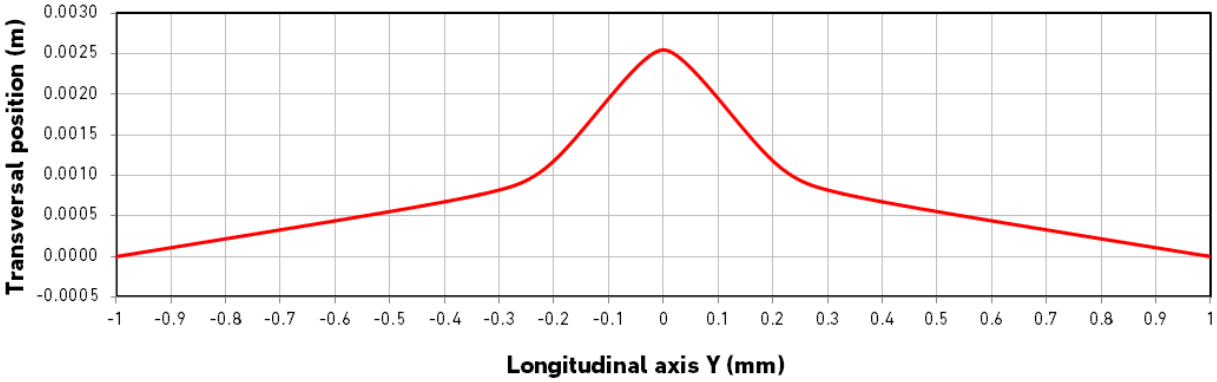

Figure 9: Map of the transversal excursion of electrons along the 3-pole-wiggler.

The maximum excursion of electrons is 2.5 mm off axis, so the beamline should be aligned according to the transversal position of the photon source, and not with respect to the straight section axis.

Effect on machine dynamics

A device as described above, placed in a straight section of a storage ring, has two types of effect on the electron beam:

- In first order, multipolar components of the magnetic field of the insertion device introduce perturbations to the ideally closed electron orbit and are determined by 1st and 2nd field integrals. This effect has been minimized in our design and, if necessary, can be corrected further by correction coils or magic fingers. This last option is recommended only in the case of fixed-gap operation. Correction coils will be needed if the device will be operated at varying gap values.

- A second order effect originates from electrons that travel at a certain distance from the nominal electron trajectory, see a slightly different magnetic field which may lead to electrons getting kicked out of the bunch. Given the fact that the electron beam is extended transversally (horizontally and vertically), this effect should be evaluated. This is done via so-called kickmaps, that represent in a 2D matrix the kicks received by electrons positioned out of the nominal trajectory.

First order effects: multipoles

The multipolar content of the 3-pole-wiggler has been computed from the field-map. The first field integral along the transversal axis is shown in Figure 10 below and the result of the fit procedure to find high order multipolar components is shown in Figure 11.

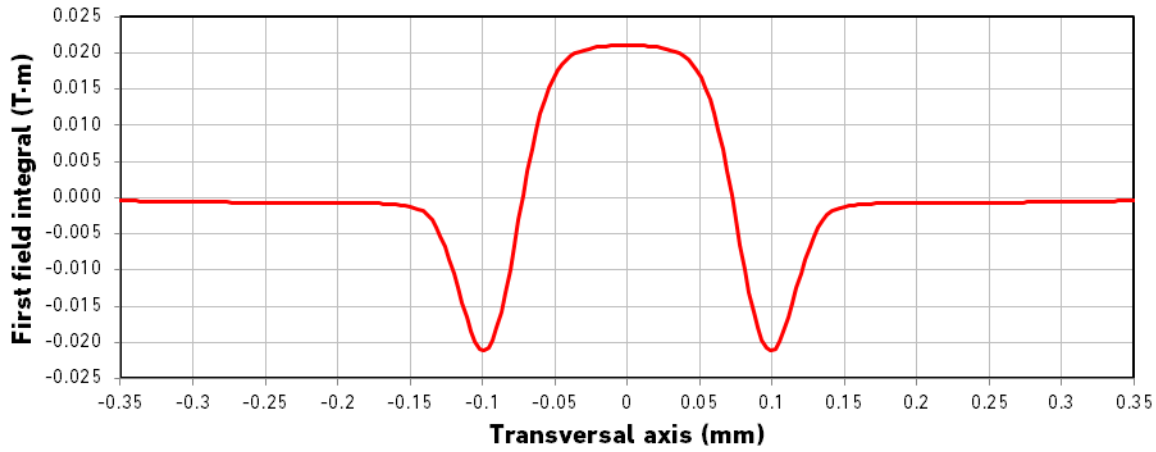

Figure 10: Field integral of the proposed 3-pole-wiggler along transversal axis

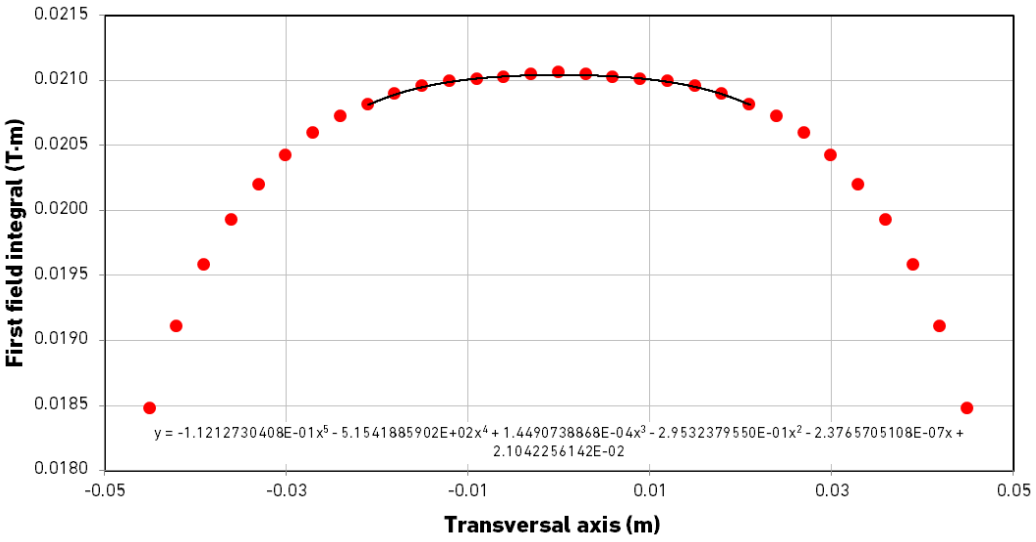

Figure 11: Field integral of the proposed 3-pole-wiggler along transversal axis in the range ±50 mm and multipole fitting in the range ±20 mm

Table 2 shows the resulting values for the multipolar field components. The values listed are reasonably small, so the effect of the 3-pole wiggler on the overall electron orbit is acceptable.

Multipole	Value
Dipole	$+2.1042 \cdot 10^{-02}$ T·m
Quadrupole	$-2.3765 \cdot 10^{-07}$ T
Sextupole	$-2.9532 \cdot 10^{-01}$ T/m
Octupole	$+1.4491 \cdot 10^{-04}$ T/m^2
Decapole	$-5.1542 \cdot 10^{+02}$ T/m^3
Dodecapole	$- 1.1213 \cdot 10^{-01}$ T/m^4

Table 2: Multipolar component of field generated by 3-pole-wiggler

Second order effects: Kickmaps

We have computed the horizontal and vertical kickmap using the RADIA code. Results shown in Figures 12 and 13, show that within the bunch volume the kickmaps are sufficiently flat.

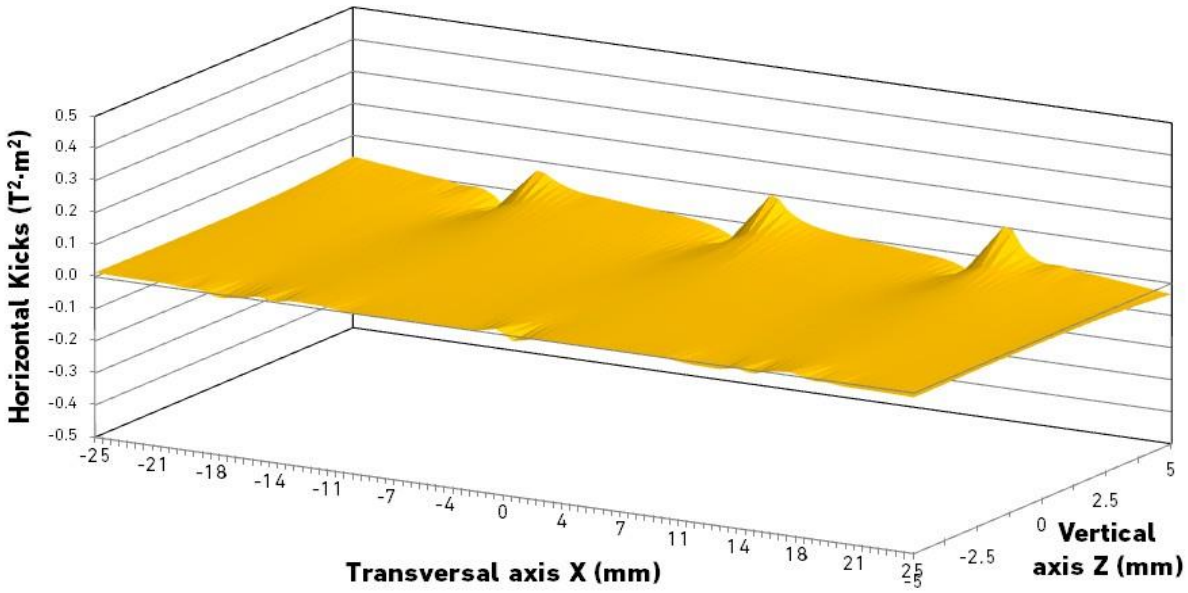

Figure 12: Horizontal kickmap.

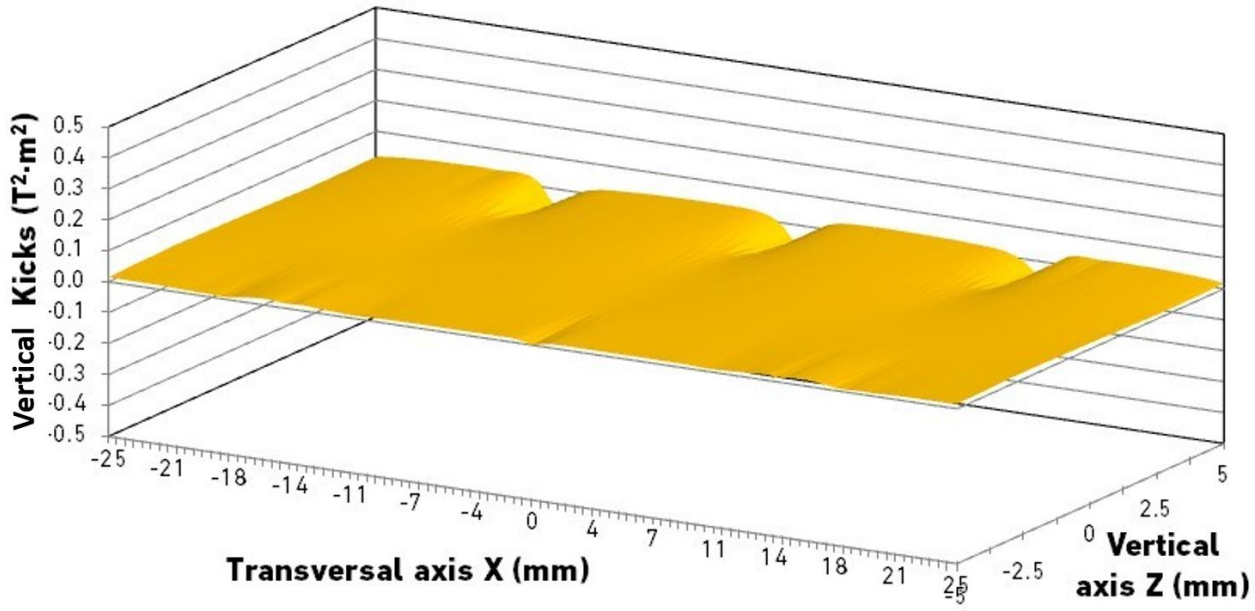

Figure 13: Vertical kickmap.

Beam dynamics and dynamic aperture

A comprehensive study of the effect of this insertion device on the dynamics of the electron beam has been reported in deliverable D3.1 of this project.

Beam dynamics studies by M. Attal (Sesame) [5] based on linear optics, dynamic aperture calculations and frequency map analysis show that the impact of the higher order multipoles generated by the ALBA 3PW-3 design can be tolerated by the machine and produce only a small dynamic perturbation at the operating energy of 2.5 GeV. The main concern for the earlier versions was for the high order multipoles, mainly the decapole component, which caused a severe reduction of the dynamic aperture. In the final version (3PW-3) these high order multipoles have been strongly reduced producing a dynamic aperture larger than the physical (vacuum chamber) aperture, see Fig.14.

The calculations of the nonlinear beam dynamics, which used frequency map analysis, showed that the impact of these high order multipoles on the nonlinear beam dynamics is tolerable and produces only a small dynamic perturbation in the aperture region needed for the beam.

During injection (at energy of 0.8 GeV), the gap of the 3-pole wiggler can be opened in order to reduce the peak field and achieve the same acceptable effect on beam dynamics as at the operating energy.

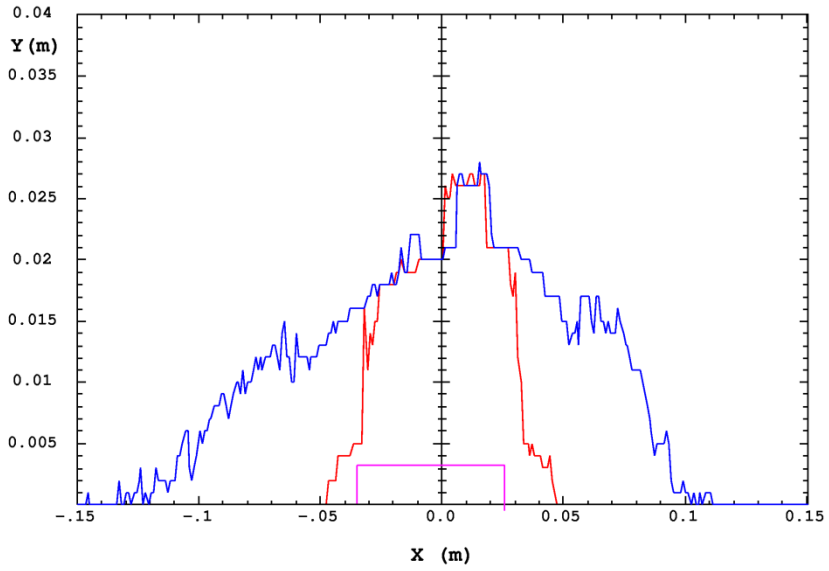

Figure 14: Dynamic aperture without (blue) and with (red) sextupole, decapole, and 14-pole components for chromaticities $\kappa_{x,y}$ = 6, 7. The magenta line represents the physical beam aperture.

The technical specifications and the fabrication characteristics of the magnet structure and the individual blocks will be reported in Deliverable 3.4 which will be the base for the tender procedure.

Spectrum of the photon beam generated by the 3-pole wiggler

The spectrum of the photon beam emitted by the 3-pole wiggler has been computed using the SPECTRA code [3], assuming an aperture of 4 mrad (h) x 1 mrad (v). Figure 15 shows the result.

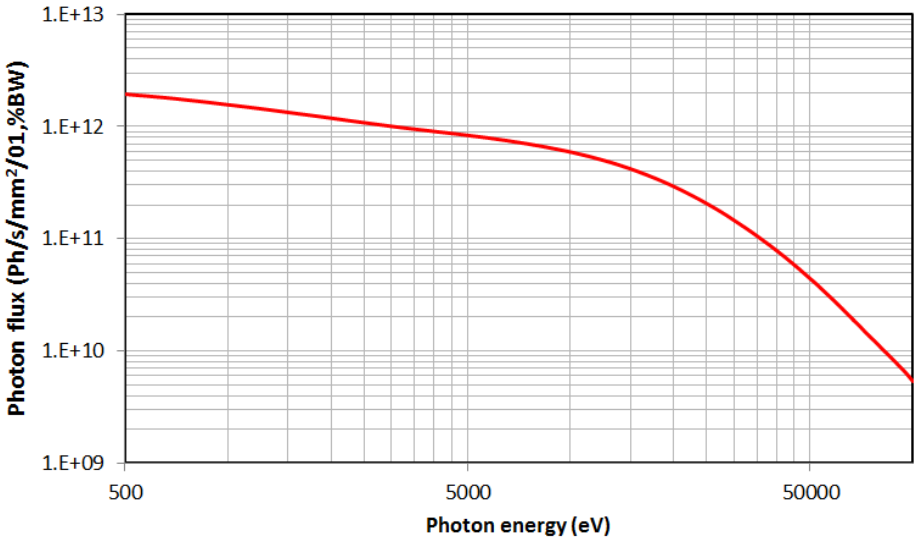

Figure 15: Emission spectrum of the 3-pole-wiggler at minimum gap through a horizontal aperture of 1 mrad.

THE ESRF WIGGLER ASSEMBLY

A 3 Tesla permanent magnet wiggler was built at the ESRF in 1999. It was primarily a design study but also foreseen and used as a possible replacement of a 4 Tesla wavelength shifter in the ID15 straight section (ESRF High Energy beamline) [6,7] . The device can be considered as two successive 3-pole wigglers (see Figure16).

Figure 16: The 3 Tesla Asymmetric wiggler installed in the ID15 straight section

The wiggler was operated with a minimum gap of 11 mm. Figure 17 shows the vertical magnetic field measured at minimal gap of 11 mm.

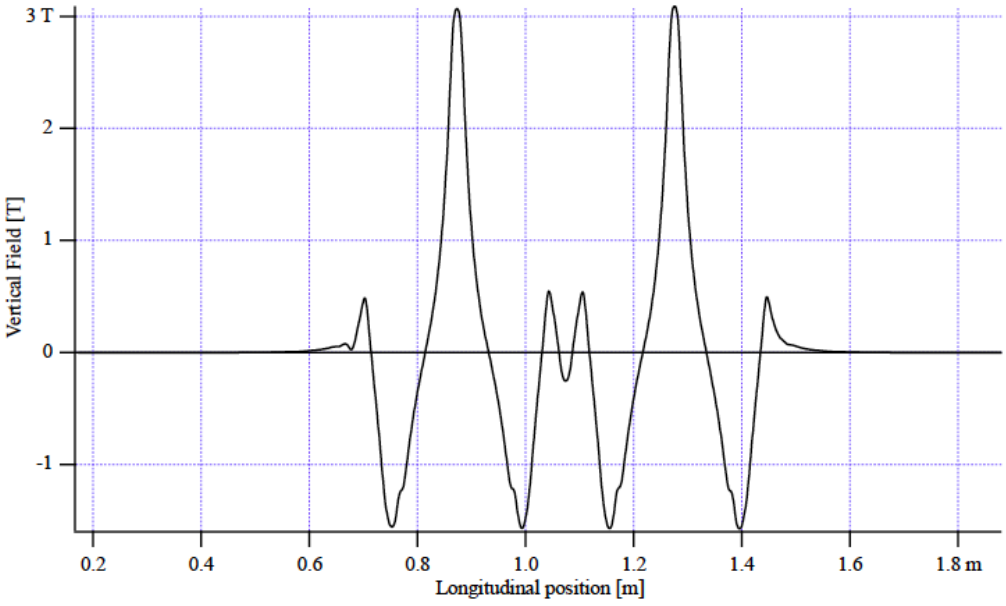

Figure 17: Measured vertical field of the ESRF wiggler assembly for a gap of 11 mm.

The device was installed in the ID15 straight section in October 2001 and operated for about 7 years, it was removed from the ring in May 2008.

With the existing parts (and some minor mechanical adaptations) three different magnetic configurations can be built which will, together with their respective photon beam properties, will be presented in what follows.

Structure of the magnetic assembly

The magnetic structure of the ESRF wiggler assembly is described in [6], the engineering details are depicted in ESRF drawings 85802058 to 85802187.

The wiggler is in fact built with four independent modules. Figure 18 shows the top view of one module. The length of one module is about 380 mm, the width is 165 mm, and the height is 157 mm.

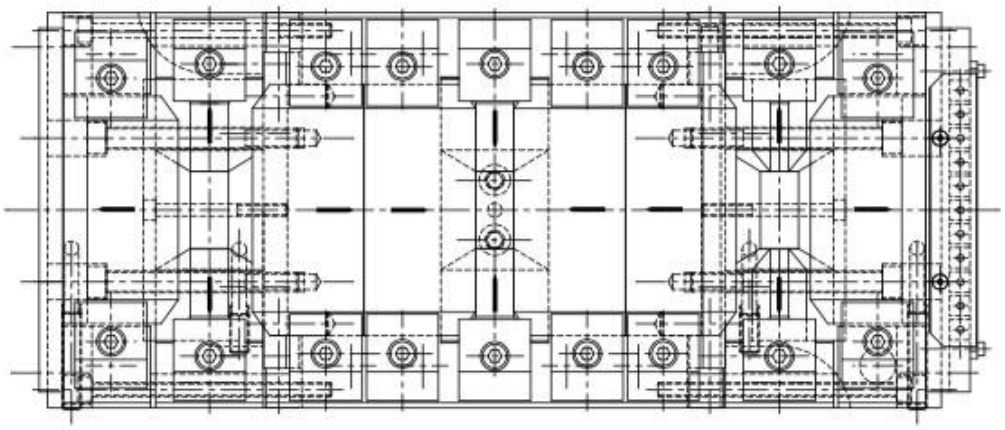

Figure 18: Upper view of one ESRF 3 T wiggler module

Each module can be separated into three self-contained parts, the central part and the two side parts. The central sub module can be considered as a dipole reaching a peak field of 3 T with two complementary central modules mounted with a gap of 11 mm.

The side sub modules allow some mechanical flexibility to tune the position and size of the magnetic blocks, they are used for controlling the field integral of the complete assembly.

With these components, one can develop three different possible magnetic configurations which shall be analyzed further in what follows:

- **3-pole wiggler (3PW):** similar to the aforementioned ALBA design: This is *a priori* the most straight forward structure, however, the side modules will very likely need to be adapted to the need for reducing the side peak field while keeping the linear integral as small as possible.
- **Super-bend magnet (SBM):** Using only the central module would constitute a super-bend with a maximum field of 3 Tesla. This concept has been abandoned already in March 2019 and therefore shall only be mentioned for the sake of completeness.
- **Two-pole wiggler (2PW*)*:** the structure of the exiting assembly can (with some modifications to the non-magnetic mechanical parts) be modified to build a 3 Tesla 2-pole wiggler.

Figure 19, 20 and 21, respectively, show the magnetic models for the three different options.

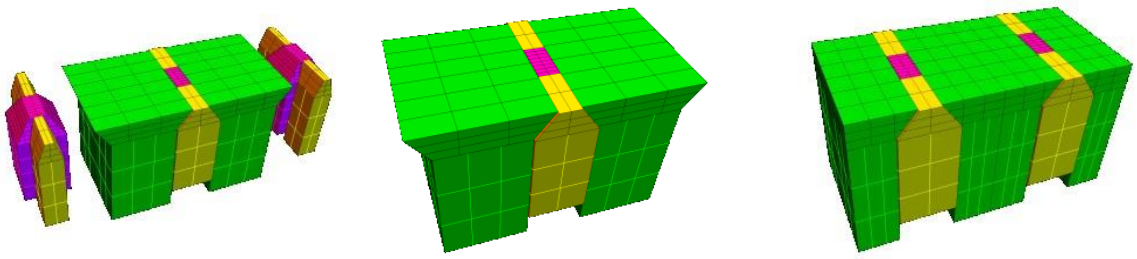

Figure 19: 3-pole wiggler model *Figure 20: Super-bend model* *Figure 21: 2-pole model*

The magnetic field

Based on the magnetic models, the magnetic field for the three configurations has been computed with RADIA. For all three cases, a field description including the part of the magnetic field of the two dipoles on either side of the straight section is included (this is necessary for evaluating for example the horizontal profile of the photon beam or to anticipate the superimposition of sources placed at different longitudinal distances.). For the dipole field a simple 3D model was used to arrive at an acceptable description of the fringe field. The distance between the edge of the dipoles is assumed

to be 7 m. Figure 22 shows the resulting vertical magnetic field for the three cases. The 2PW is shifted downstream from the centre of the straight section (here 0.8 m) to allow the integration of two low field steerers to compensate the resulting horizontal offset on the electron beam and to reduce as well the emission from the upstream dipole.

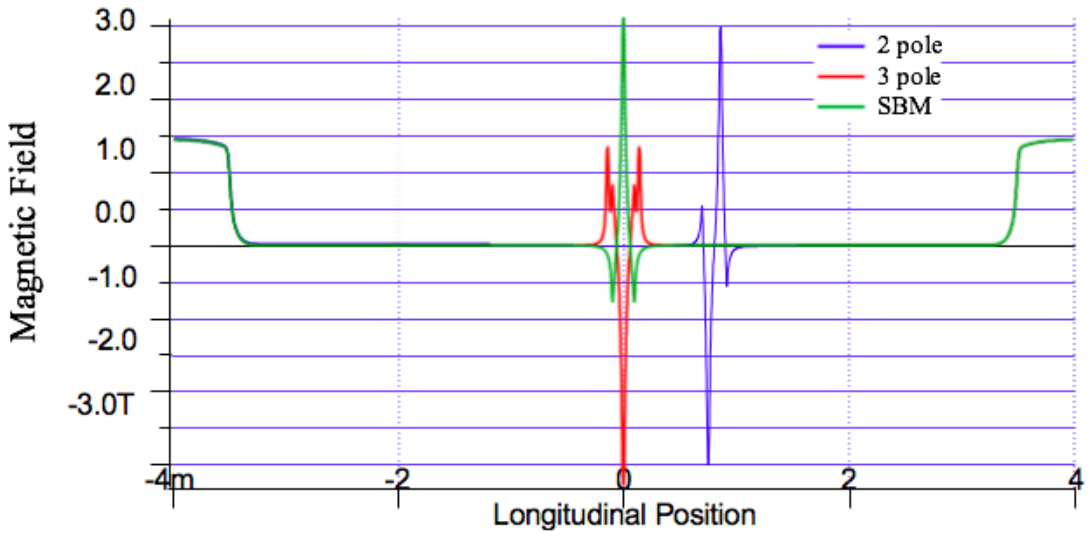

Figure 22: Vertical magnetic field model for the three different structures (green: SBM, red: 3PW and blue, 2PW)

The permanent magnet material is of type NdFeB with a remanence of 1.24 T and a relative permeability of 1.05 (1.15) parallel (perpendicular) to the easy axis. The pole material is a classical high saturation FeCo alloy with 49% Fe, 49 % Co and 2 % Vanadium.

Electron beam motion

Electron beam parameters

The parameters of the electron beam are those of a short straight section within the SESAME storage ring (see table 3) It allows a correct description of the beam envelope in the drift space between the focusing magnets.

Parameter	Value
Energy [GeV]	2.5
Current [mA]	400
Emittance H/V [nm]	25.74/0.2574
Beta value at middle of straight H/V [m]	13.27/0.77
Horizontal dispersion [m]	0.533
RMS Energy spread [%]	0.1073
Horizontal/Vertical RMS beam size [μm]	791/14
Horizontal/Vertical RMS beam divergence [μrad]	44/18

Table 3: SESAME electron beam parameters at the short straight sections

Source points

In this section we shall investigate in more detail the electron motion within the magnetic field of the aforementioned three possible magnetic configurations. Plotting the total magnetic field at the source point vs. the horizontal observation angle (Figure 23) yields information on the photon emission of the magnetic structure (emission direction and profile, eventual superposition of several source points).

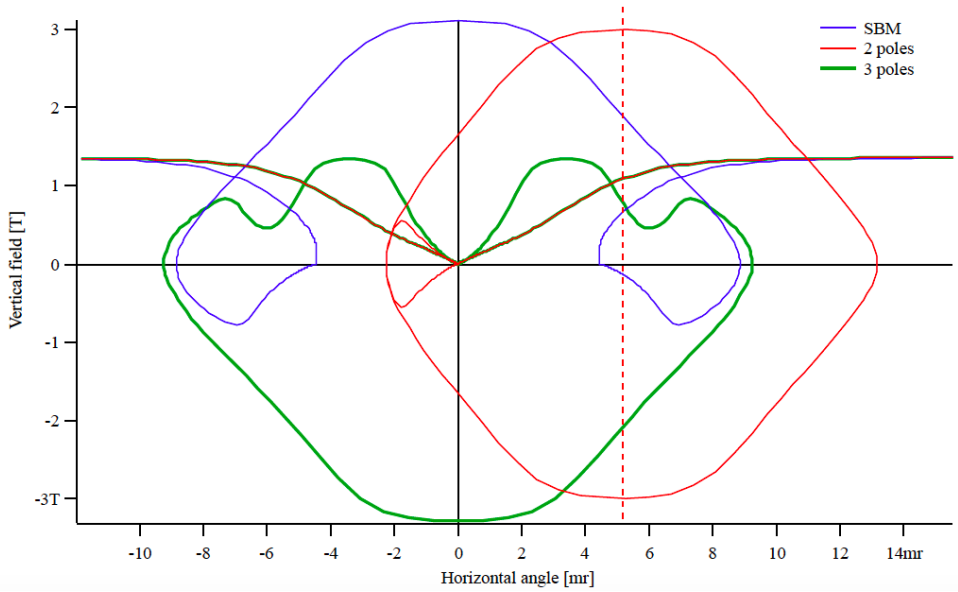

Figure 23: Magnetic field versus horizontal angle for the three magnetic configurations: blue: SBM, red: 2PW, green: 3PW

- For the SBM configuration (blue) , as expected, there is one central range of emission from only one source point centred at 0 mrad with a width of around 9 mrad (the deflection angle). However, the magnetic field at the entrance and the exit of the SBM configuration leads to side peaks of emission centred at +7 mrad and -7 mrad. As for these emission directions the magnetic field is low, these peaks will be visible only in the regime of low photon energies (< ~ 7 keV).

- For the 2-pole wiggler configuration (red), the emission is centred at a horizontal angle of about 5.5 mrad, the x-ray fan points outward the axis of the straight section. There is only one additional source point originating from the upstream dipole (around -1 mrad), which leads to a slight gradient in the horizontal profile of the total x-ray beam. The x-ray beam generated by the second dipole closer to the beamline is not in the field of view.
- For the 3-pole wiggler configuration (green), three source points come into play: emission from the central pole, from one side pole and one from an adjacent dipole (the downstream dipole being much closer to the beamline than the upstream dipole). One can expect a significant asymmetry in the horizontal profile of the total x-ray beam for photon energies below 15 keV.

The transverse horizontal trajectory of the electron beam is shown in Figure 24. For the SBM and the 3PW configuration, the effect on the electron trajectory is zero, while for the 2-pole wiggler there is a net horizontal 1 mm offset induced on the electron beam orbit, which needs to be compensated by two low field steerers installed in the straight section.

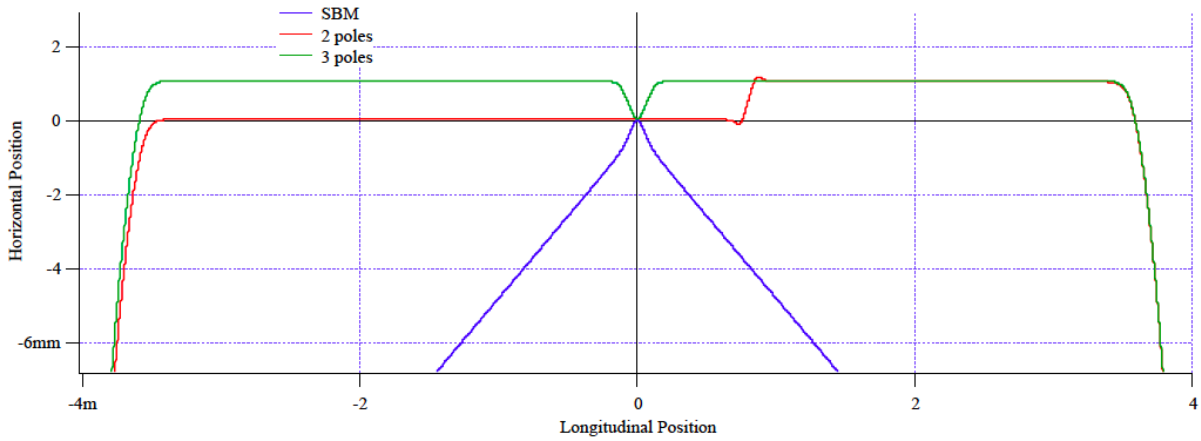

Figure 24: Electron trajectory in the horizontal transverse plane for the three source types.

The photon emission

Figure 25 shows the photon flux for the three magnetic configurations, calculated with the SRW code. The emission of the 3-pole wiggler features a strong contribution at lower energies, originating from the dipole magnet contribution (including the edge field). The spectrum emitted by the 2-pole wiggler configuration is about a factor of two more intense compared to the 3PW due to the fact, that two 3 T magnets contribute in this case.

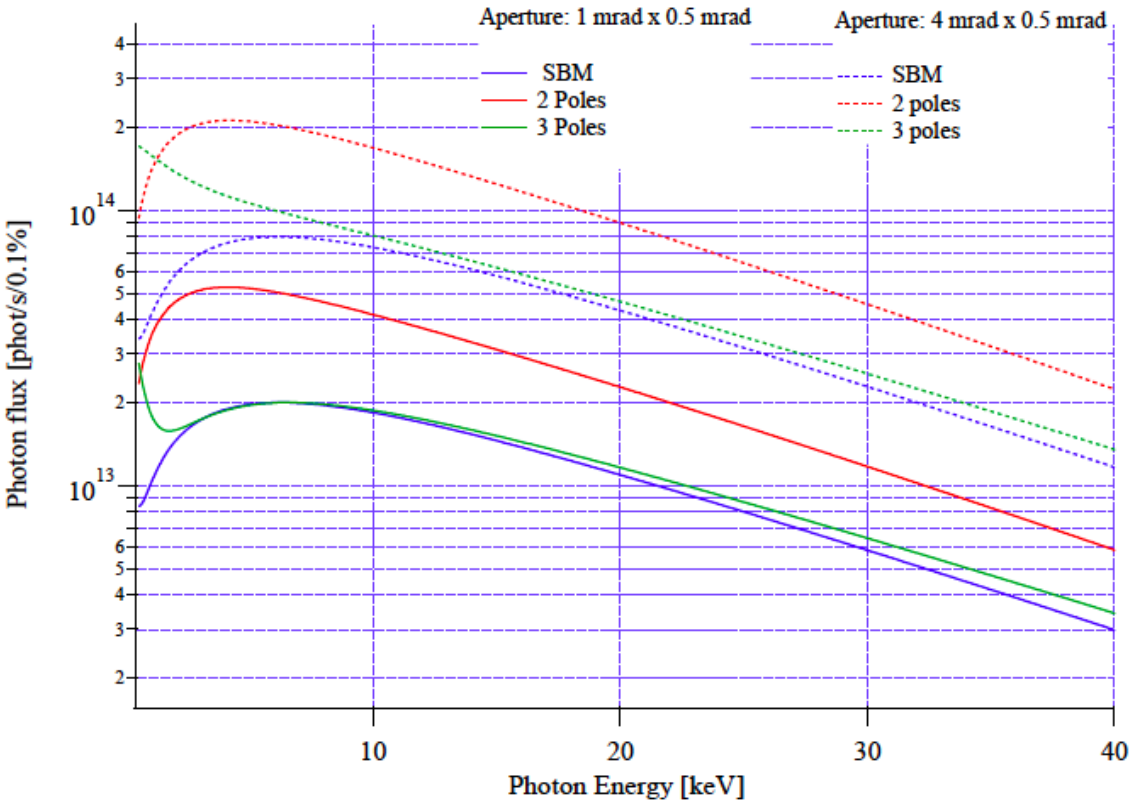

Figure 25: Photon flux integrated over the angular aperture of 1 mrad (plain lines) and 4 mrad (dotted lines) horizontally for the three magnetic configurations. The vertical angular aperture is 0.5 mrad in all cases.

Transverse profile of the photon beam.

The transverse profile of the photon beam is evaluated at a distance of 10 m from the middle of the straight section in terms of photon flux per unit surface (i.e phot/s/0.1% bw/mm^2). Figure 26 shows the resulting horizontal profile for the three source types (A: SBM, B: 2PW, C: 3PW). Similarly, Figure 27 presents the vertical profiles of the photon beam.

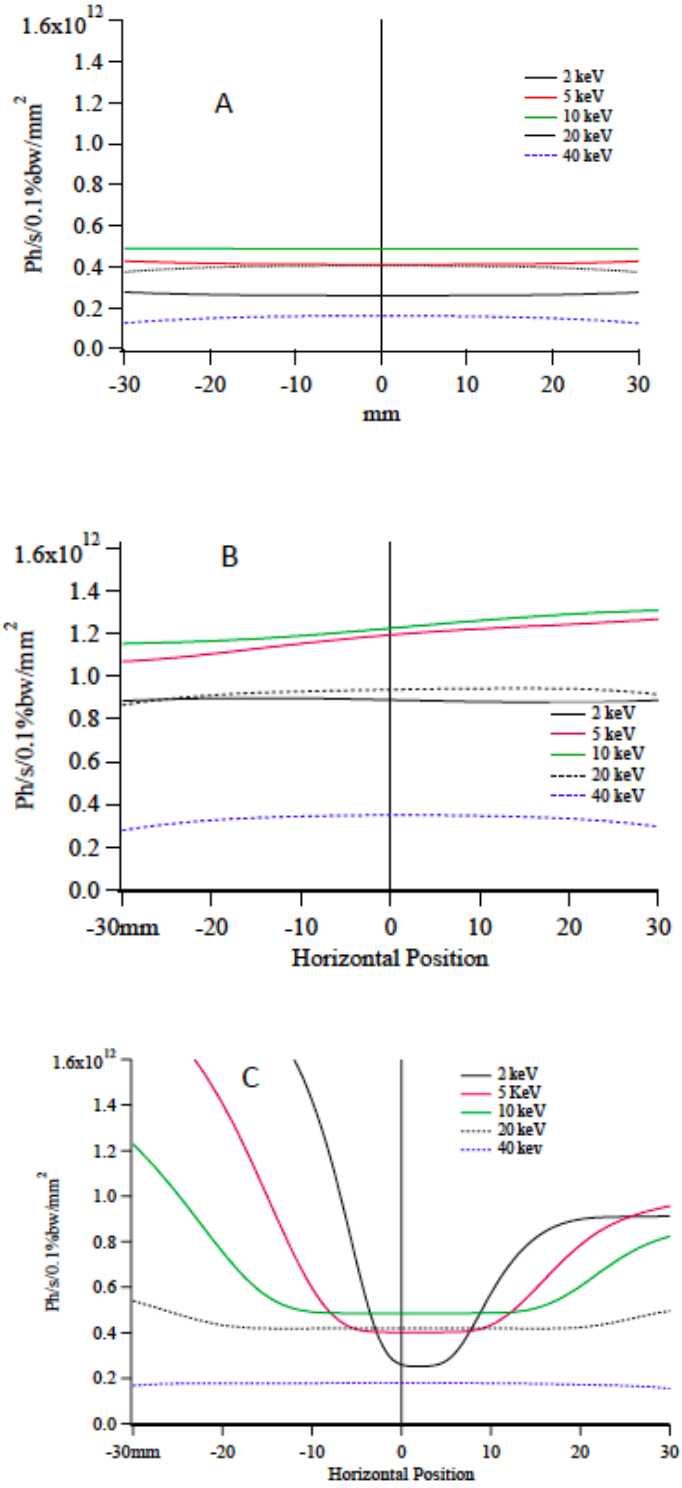

Figure 26: Horizontal profile of the photon beam at 10 m from the centre of the straight section for different energies. A: SBM, B: 2PW and C: 3PW

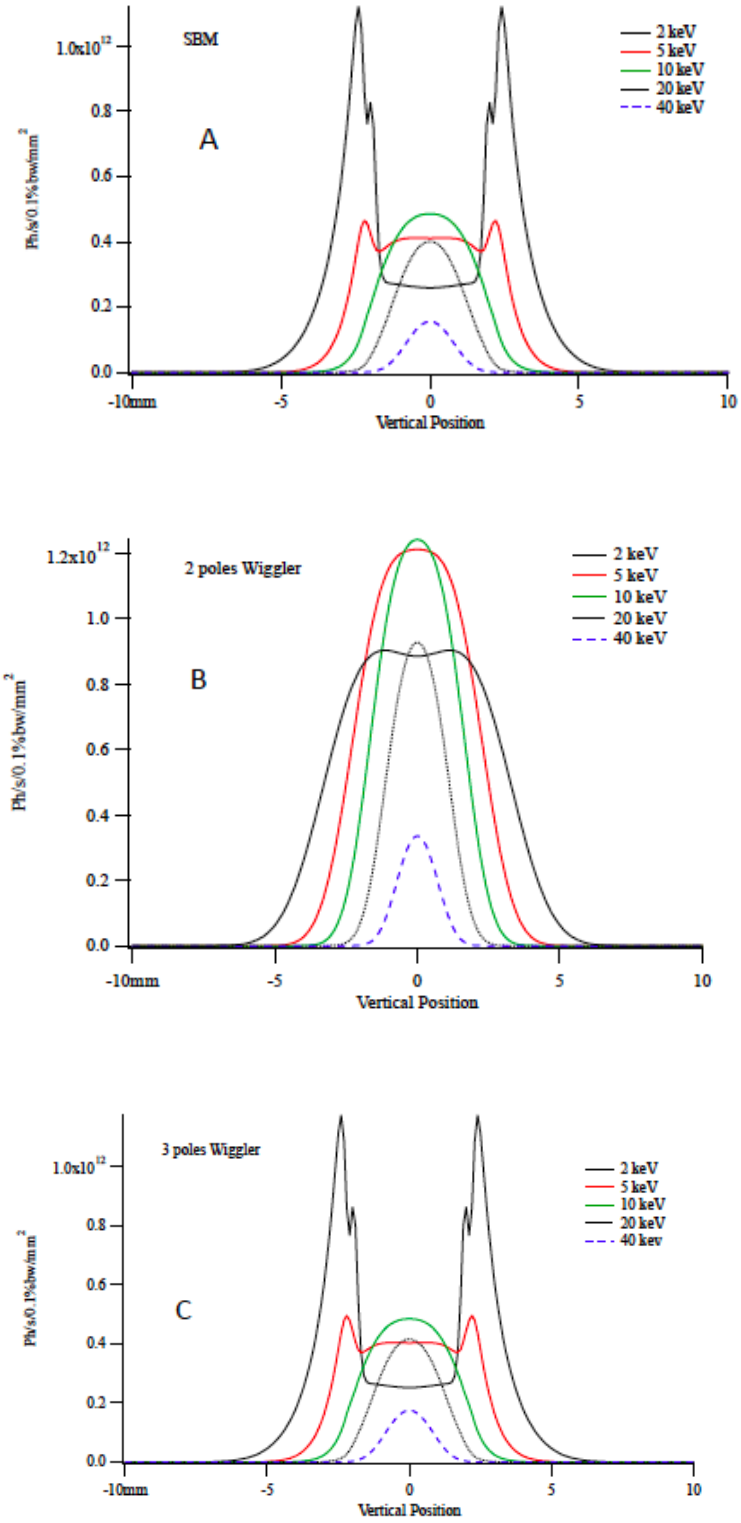

Figure 27: Vertical profile of the photon beam at 10 m from the centre of the straight section for different energies. A: SBM, B: 2PW and C: 3PW

From the results shown in Figures 26 and 27, one can conclude:

- The best homogeneity of the horizontal profile is obtained for the SBM case.
- For the 2PW configuration, the horizontal profile includes (in the energy range between 5 keV and 10 keV) a slight gradient due to the contribution of the edge field from the first dipole, it may depend on the refinement of the fringe field for this dipole.
- The horizontal profile of the 3PW configurations is not homogeneous primarily due to the contribution of the side poles and that of the two dipoles which bring a significant left/right asymmetry. A modification of the side field may change the result noticeably. However, depending on the horizontal range, the contribution of the two dipoles will always remain visible in the low photon energy.
- For the 3PW as well as the SBM configuration, the vertical profiles are relatively similar and exhibit side peaks due to the side field in both cases. The 2PW's vertical profile does not show such a feature due to the large distance between the upstream dipole and the 2PW.

Source size

The transverse source size is determined from the 2D structure generated when projecting the emitted light along the electron trajectory on a reference plane placed longitudinally at the middle of the source of interest. Different methods used may lead to different results especially for superimposed sources as in our case for the 3PW and the 2PW configuration. For example a 2D gaussian fit (which was used in our case) and an analysis based on second order moments lead to different results.

Transverse horizontal plane

Figure 28 shows the projected horizontal motion (projection of the points of the electron trajectory along the tangent to these points) of the electrons versus the horizontal angle in the transverse plane at the center of the source (blue and left axis) for the three source types (A: SBM, B:2PW, C:3PW). Because the radiation is emitted tangentially to the electron orbit, this allows to estimate the photon distribution at the source. It is also practical to add the field versus the horizontal angle (red axis). By limiting the analysis to the angular acceptance of ± 2 mrad, the field can be assumed to be constant at ~3 T. We confine the analysis to the high photon energy range (> 15 keV) From Figure 28 the following conclusions can be drawn:

- For the SBM case (A) and an angular acceptance lower than about 4mrad centered on the axis (0 mrad), the contribution of the horizontal motion to the source size is negligible compared to the size of the electron beam (790 µm RMS). The source size is therefore entirely dominated by the size of the electron beam.

- For the 2PW case (B), the projected motion shows the expected two separated branches. Moreover, the contribution of the beam motion to the size of the source depends on the observation angle. For a centered observation (i.e at the center of the x-ray fan) and angular acceptance lower than ~ 4 mrad, the two branches are separated by an average distance of $2a \approx 600\ \mu m$, the source size can be estimated according to [2] :

$$\Sigma_x \approx (\sigma_x^2 + a^2)^{\frac{1}{2}} = 845\ \mu m = 1.07\ \sigma_x$$

with σ_x being the horizontal RMS size of the electron beam, the increase in the source size due to the two separated poles is relatively moderate. Note that the equation is a simplification of the expression derived in reference [2] which includes a third term link to the single electron emission (which is photon energy dependent). This term is neglected here.

Exploring further the diagram of Figure 28 B, one can locate transversally the position of the upstream dipole source which is at an offset of about 22 mm compared to the 2PW source point as depicted in Figure 29 using an angular acceptance range of ± 2 mrad.

- For the 3PW, provided that the angular acceptance remains small (in the range ± 2mrad) and the considered photon energy issufficiently higher than the critical energy of the side poles, the horizontal source size is that of the electron beam.

Transverse vertical plane

Within the same framework as for the horizontal plane, also the vertical source size is dominated by the size of the electron beam for all three cases and one arrives at a value of $\sigma_Z \approx 14\ \mu m$.

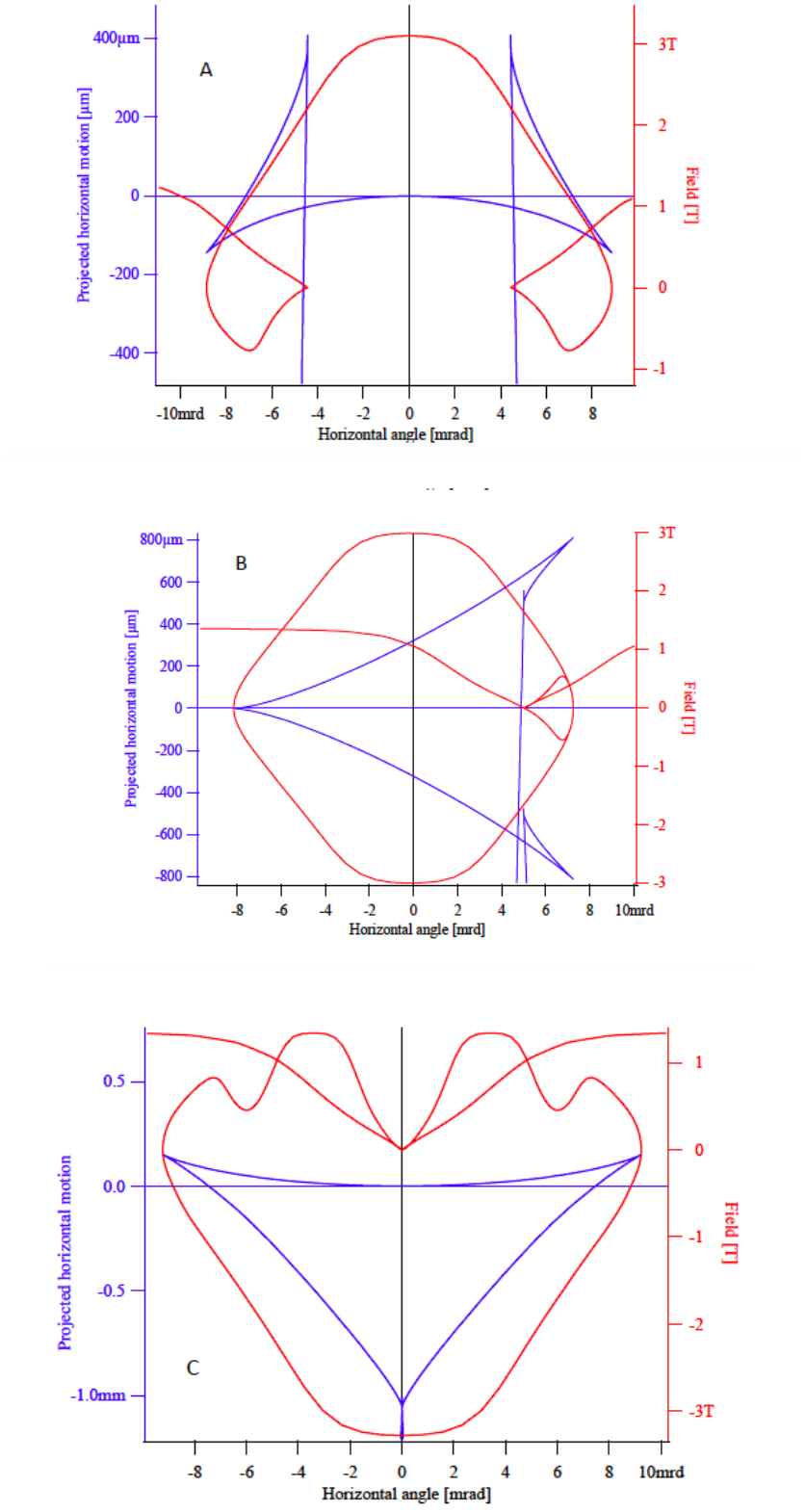

Figure 28: Projected horizontal electron motion (blue) and vertical field (red) versus horizontal angle (blue) for the SBM (A), the 2PW (B) and 3PW (C).The projection plane is located at the middle of the source.

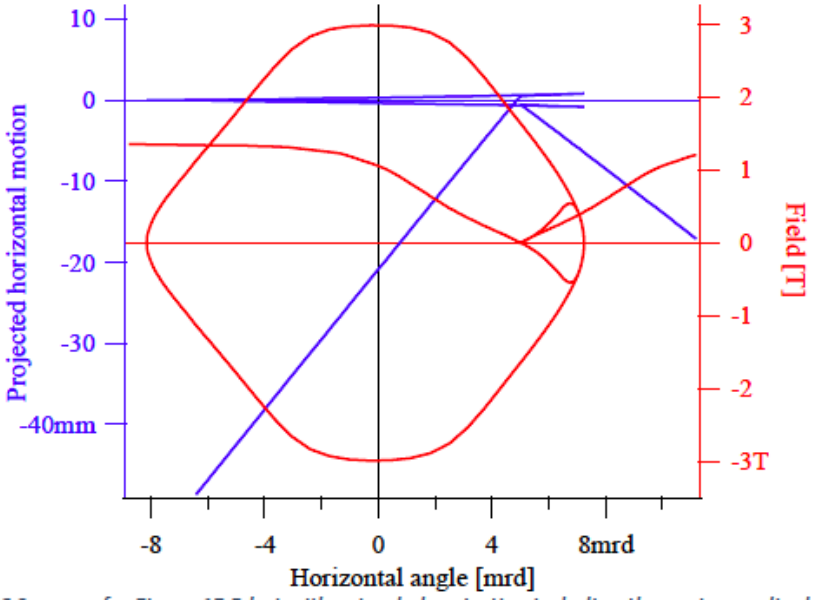

Figure 29: Same as for Figure 28 B but with extended projection including the upstream dipole source

Heat load considerations

Figure 30 shows the power density of the white beam at 10 m distance from the center of the straight section for the tree types of source: SBM (A), 2PW (B) and 3PW (C). The impact of the downstream dipole (left side on the images) on the horizontal homogeneity is clearly visible for the SBM and 3PW case. For the 2PW , since the x-ray fan is shifted in angle outward from the axis of the straight section, the downstream dipole does not contribute to the 2D profile of the wiggler. The power density reaches 6 W/mm^2 for the 2PW configuration.

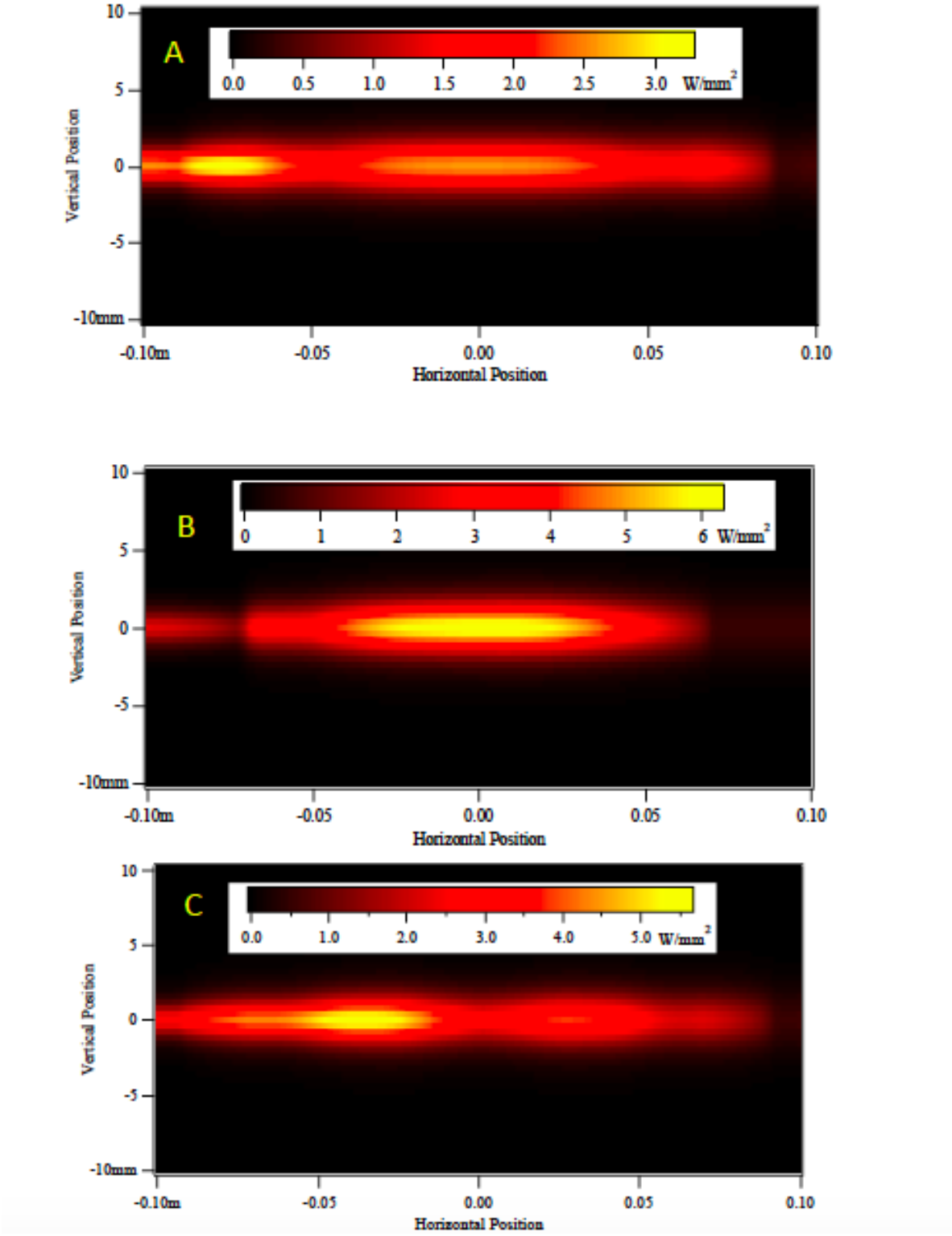

Figure 30: Power density of the white beam at 10 m from the middle of the straight section for the three source types: SBM (A), 2PW (B) and 3PW (C)

Status of the ESRF 3T wiggler assembly

The 3T wiggler assembly consists of four modules stored in separate boxes. The modules are shown in the photos below. A few chips are visible near the magnet corners but the overall state is rather acceptable, in particular, there is no observable surface corrosion at the magnet surface.

Module # 1

Module#2

Module # 3

Module # 4

SUMMARY AND CONCLUSIONS

A first decision on the type of source has been taken at the BEATS kick-off meeting in March 2019. The concepts of a super-bend and a multipole wiggler were rejected due to their strong impact on the storage ring. Therefore, it was decided to use as source a 3 pole wiggler with 3 T field to be installed in one of the 'short' straight sections of the SESAME ring. Deliverable 3.1 summarizes the underlying investigations.

In the following months different 3-pole wiggler models have been proposed (3PW-1, 3PW-2, 3PW-3) and the possibility of refurbishing the ESRF prototype of a 3T wiggler in a 2-pole wiggler configuration [6], which potentially can provide a factor of 2 more flux with respect to the 3-pole design.

Two main concerns were raised when considering the option of reusing the existing ESRF wiggler assembly:

- Due to its large dimension, the magnet cannot be installed in the short straight section of SESAME "as is", a complete disassembly and reassembly of the device would be necessary.
- The strong commitment of the ESRF Insertion Device Group with the ESRF EBS upgrade programme and the corresponding workload in combination with the BEATS internal deadline for the procurement of the source makes it unrealistic to complete the study of the contribution of nonlinear multiple components of the magnet, and consequently the impact on the electron beam dynamics on time.

To avoid the risk of slowing down the project and in view of the fact that the ALBA 3-pole wiggler design fulfils all requirements it was decided, in consultation between the BEATS Steering Committee and the SESAME scientific and machine Management to use the ALBA design as x-ray source for the BEATS beamline at SESAME.

REFERENCES

1) R. Bartolini, 'Update from WP3', BEATS kickoff meeting, Sesame 12 - 13 March 2019
2) J. Campmany, 'The Photon Source for the BEATS beamline at SESAME', BEATS kickoff meeting, Sesame 12 - 13 March 2019
3) WP3 Working Group, 'BEATS WP3 – Decision on the type of wiggler', 30 September 2019
4) J. Campmany, 'Technical specifications and conceptual design of a 3PW photon source for the BEATs beamline at SESAME syncrotron' *ALBA Project Document* AAD-IDBEATS-A-0002, 29 March 2019, Rev. 1, 13 June 2019, Rev. 2, 16 July 2019.
5) M. Attal, 'Impact of the Proposed Wavelength Shifter on SESAME Beam Dynamics', May 31, 2019, updated on June 27, 2019, latest version August 27, 2019
6) Nuclear Instruments and Methods in Physics Research A 421 (1999) 352–360
7) J. Chavanne, '3T Wiggler @ ESRF: Status and possible updates', ESRF 02-IDM-2019, July 2019